Available online at http://scik.org
Commun. Math. Biol. Neurosci. 2025, 2025:59
https://doi.org/10.28919/cmbn/9225
ISSN: 2052-2541

INVESTIGATING THE EFFICACY OF INSECTICIDES IN CONTROLLING THE SPREAD OF TUNGRO VIRUS IN RICE PLANTS: A MATHEMATICAL MODELING APPROACH

DANI SUANDI[1,*], MOCH. FANDI ANSORI[2], DIPO ALDILA[3], VISKA NOVIANTRI[4], ENCENG SOBARI[5], NADIRAH BINTI MOHD NASIR[6]

[1]Computer Science Department, School of Computer Science, Bina Nusantara University, Jakarta, 11480, Indonesia

[2]Department of Mathematics, Faculty of Science and Mathematics, Universitas Diponegoro, Semarang, 50275, Indonesia

[3]Department of Mathematics, Universitas Indonesia, Depok 16424, Indonesia

[4]Mathematics Department, School of Computer Science, Bina Nusantara University, Jakarta, Indonesia

[5]Study Program of Food Crop Production Technology, Department of Agriculture, Subang State Polytechnic, West Java, Indonesia

[6]Centre for Mathematical Sciences, College of Computing and Applied Sciences, Universiti Malaysia Pahang Al-Sultan Abdullah, 26300, Pahang, Malaysia

Abstract. The rise in population and robust economic expansion have led to a heightened need for food, energy, and water resources. In such circumstances, food security becomes an indispensable necessity for human survival. However, while striving to uphold food security, we frequently encounter the challenge of crop failure due to pest infestations, particularly green planthoppers. These infestations can lead to a reduction in both the quality and quantity of crop yields, and they also have the potential to disseminate the destructive tungro disease virus, further compromising crop health. Utilizing a mathematical modeling approach, a complex five-dimensional nonlinear

*Corresponding author
E-mail address: dani.suandi@binus.ac.id
Received March 04, 2025

system of differential equations is formulated to depict the intricate dynamics between rice plants and planthopper pests in the transmission of the tungro virus. This approach is adopted to investigate the effectiveness of control measures in curtailing the transmission of the tungro virus via planthopper pests. The model includes two control measures, which are the application of insecticides and the removal of infected plants, aimed at mitigating the virus's transmission. We conducted stability analysis and derived the basic reproduction number formula ($\mathscr{R}_0$) to examine the qualitative behavior of the model. Furthermore, the stability of the interior equilibrium was analyzed using the Monte Carlo method, allowing for a robust evaluation of system dynamics under varying parameter uncertainties. As the basic reproduction number is influenced by the two aforementioned controls and endemic conditions emerge when this number exceeds one, we performed a sensitivity analysis to assess the impact of these control measures on reducing the $\mathscr{R}_0$ value and infected compartment. Subsequently, we conducted an optimal control investigation to assess the efficacy of implementing these two control measures by developing various scenarios. Our results indicate that implementing both insecticide application and the removal of infected plants together is considerably more effective than implementing these control measures separately.

Keywords: tungro virus; control optimal; stability analysis; sensitivity analysis; Monte Carlo simulation.

2020 AMS Subject Classification: 34H05, 34A12, 37N25, 97M10, 97M60.

1. Introduction

Food is a fundamental biological necessity for all individuals, playing a crucial role in fulfilling nutritional requirements, maintaining health, and fostering sustainable productivity. Ensuring every person has access to an adequate, safe, nourishing, and reasonably priced food supply represents a fundamental human entitlement. The significance of food also resonates in the pursuit of Sustainable Development Goals, particularly in the endeavor to eradicate hunger. The growth in population has significantly influenced the continuously rising demand for food. This has implications for the food supply, necessitating a continuous increase in its volume. Moreover, the food industry is a sector capable of influencing the advancement of the national economy [1, 2]. The economic expansion in Asia experienced instability due to the impact of the COVID-19 pandemic several years ago. The COVID-19 pandemic has burdened the agricultural sector by disrupting labor availability and market access, leading to additional economic losses [3, 4]. As a consequence, the regional economic growth in Asia is anticipated to decelerate, with a projected rate of 7.1% in 2021 and 5.4% in 2022. This has given rise to various challenges, particularly within the realm of agriculture, which is a pivotal sector in the development of Asian economies.[5, 6]. In regions like Assam, India, the lockdowns resulted

in substantial crop losses due to halted agricultural activities, with large farms experiencing up to 71.69% loss [4]. Despite these challenges, the agricultural sector in India showed resilience, contributing positively to GDP, although it faced significant hurdles [7].

Although COVID-19 has a broader economic impact [8], organisms like algae, fungi, bacteria, mycoplasma, and viruses on plants are more destructive in the agricultural sector, particularly in rice cultivation [9]. COVID-19 does not directly damage crops but disrupts the agricultural supply chain. Mobility restrictions during the pandemic caused difficulties in distributing fertilizers, pesticides, and agricultural labor [8]. As a result, crop production was affected, leading to increased food prices. Its impact was global, affecting various agricultural sectors and worsening food security in many countries, especially developing nations reliant on food imports. On the other hand, plant viruses directly attack rice plants through vectors like the green leafhopper, causing total crop failure in infected fields [10]. Historical data indicates that major epidemics have caused rice production losses of up to 53% in affected districts, translating to millions of tonnes lost annually. For instance, the 2001 epidemic in West Bengal resulted in a loss of 0.5 million tonnes of unmilled rice, valued at approximately Rs 2911 million. The cumulative economic impact of these losses has escalated over the years, with significant increases in real value losses during major outbreaks [11, 12]. Similarly, rice black-streaked dwarf virus (RBSDV), transmitted by the small brown planthopper, has led to severe yield losses in rice production during outbreaks in countries like Japan, China, and Korea [13]. This virus also has the potential to destroy up to 100% of rice production in endemic regions such as Indonesia, the Philippines, and Thailand, where rice is a staple food [14]. If left uncontrolled, this plant virus could become a serious threat to national food security and lead to billions of rupiahs in losses for farmers.

Plant viruses pose a significant agriculture-related worry due to their ease of transmission and the substantial impact they bring about. The consequences of these viruses are evident in the disruptions they cause, leading to persistent reductions in agricultural production and crop quality [15]. Viruses are well-known for their propensity to infect practically every form of plant and cause significant damage to certain cultivated crops. Research indicates that there are 25 distinct virus types that can infect rice plants and directly affect crop yields economically.

Most of these viruses are transmitted by insects that either swim or feed on plant leaves [16]. The rice tungro virus, sometimes known as tungro, is a dangerous rice disease that necessitates precise management efforts. It is caused by two viruses, RTBV (Rice Tungro Bacilliform Virus) with a rod-like structure and RTSV (Rice Tungro Spherical Virus) with a spiral shape. RTBV, a pararetrovirus belonging to the Caulimoviridae family, depends on helper viruses produced by RTSV for its transmission and plays a primary role in causing severe tungro symptoms [17]. These two viruses engage with rice plants, prompting symptom expression and the development of the disease [16, 18]. Plant viruses need to be transmitted by vector organisms (insects, nematodes, zoosporic endoparasites) for their spread from plant to other plants [19]. This virus spreads by vectors, with the green leafhoppers Nephottetix virescens and N. nigropictus, as well as the striped leafhopper Roselia dorsalis, being particularly responsible.

Green planthoppers have a significant role in disseminating and transmitting the Tungro virus within rice fields [20]. Rice Tungro Bacilliform Virus (RTBV) induces symptoms like yellowing of leaves, decreased tillering, stunted plant growth, the emergence of suspended panicles, and grain browning due to incomplete filling [21]. Conversely, Rice Tungro Spherical Virus (RTSV) is a virus that contributes to the Tungro disease and is required by RTBV for transmission by green planthoppers [17, 22]. Green planthoppers undergo a three-phase life cycle, consisting of eggs, nymphs, and adults. Eggs are deposited on the midribs of rice leaves and hatch into nymphs within 7-10 days. These nymphs undergo five molting stages before maturing into adult planthoppers, which have a lifespan of 20-30 days and then lay eggs again. The damage inflicted by green planthoppers involves extracting liquid from the leaves, leading to symptoms like leaf yellowing, stunted growth, and reduced plant size. It is during this phase that planthoppers carrying the Tungro virus can transmit the virus to other plants. The Tungro disease is disseminated via infection sources like remnants of diseased plants and interaction with other susceptible host plants. Green leafhopper numbers exhibited an increase during the wet season, and the rice planting schedules were not synchronized, especially in plants receiving significant nitrogen fertilization [20].

Detecting Tungro disease in the field isn't always straightforward, as the classic symptoms may not manifest in all varieties. Tungro can be identified through tests using iodine and flour,

or by subjecting plants to insect transmission tests. However, the iodine and starch test only reveals an increase in starch levels in infected plants, making it less dependable, while the insect transmission test involves a complex procedure. On the other hand, serological techniques offer a relatively specific, sensitive, and reliable means of detecting the Tungro virus [23]. Management of plant viral diseases typically involves the widespread use of chemicals designed to target and control the vectors (such as insects, nematodes, and fungi) responsible for transmitting the viruses. Nevertheless, chemicals have notable adverse effects on both human health and the environment [15], underscoring the necessity for alternative methods to reduce chemical usage in pest and disease management. A commonly employed alternative involves harnessing plant genetic resistance, a strategy rooted in the interplay between plants and viruses within agricultural contexts [24]. Farmers utilize insecticides, including the active component Cypermethrin and pyrethroid compounds, as a preventive measure against the transmission of the tungro virus [25].

Besides the application of insecticides, managing the tungro virus involves the selection of superior seeds through breeding to develop resistant varieties [26]. Fundamentally, plant resistance to viruses hinges on the intricate interactions between plants and viruses, leading to physiological alterations and disease manifestations in plants. In response to viral infections, plants possess secondary metabolites that contribute to defensive reactions against both biotic and abiotic stressors. These secondary metabolites enhance plant resistance to viruses by regulating defense pathways. Furthermore, plant hormones, such as ethylene (ET), jasmonic acid (JA), and salicylic acid (SA), serve as immune agents, governing responses to viral infections. Candidate varieties identified as strong donors for tungro resistance, as determined by the spectrum of tungro infection rates in single-cross populations, encompass Utri Merah, Tjempo Kijik, Hundred Days T36, M1085c-10-1 (Indonesia), and F8 plants with codes PSB Rc4 x TI-11- 8, BPI Ri10 x TI-11-8, and IR64 x TI-11-8 (Philippines) [27]. Breeding lines originating from Red Utri (IRGC accession number 16680) and ARC11554 (IRGC accession number 21473) exhibited resistance to the tungro virus in the Philippines and Indonesia, but not in India [28].

A systematic literature review conducted by Amelia [29] stated that there has been limited research focused on analyzing the transmission of the tungro virus within rice plants using

mathematical modeling within 2016 - 2021. Among the 129 papers in the Dimension database, 5,000 papers in the Google Scholar database, and 374 papers in the Scopus database related to tungro viruses, merely eight of them are associated with mathematical models examining the propagation of tungro viruses. The dynamical tungro viruses spread has been modeled by eight compartments, including compartments for rice plants and green leafhoppers [30]. Moreover, this research was completed by an optimal control model based on the pesticide used [31]. An examination of mathematical models depicting the transmission of the tungro virus involving two distinct virus types is presented in [32],[33]. The exploration of insecticide control is also addressed through mathematical model analysis in [34]. Furthermore, [35] investigates the propagation of the Tungro virus within rice plants by utilizing a matrix method approach, partitioning rice plant plots into two stages: the vegetative phase and the generative phase. Additionally, [36] delves into constructing a mathematical model that incorporates biological agents and environmental factors

Among the reviewed literature on mathematical models of tungro virus transmission, interventions like the removal of diseased plants have not been incorporated and thoroughly investigated. In this examination of tungro virus spread in rice plants, we will take this factor into account. Furthermore, we will also examine the impact of pest control measures using insecticides to explore various effective scenarios. This discussion holds significant importance in establishing a comprehensive understanding for devising an optimal strategy to control the spread of tungro pests in rice plants.

2. Mathematical Formulations

Mathematical modeling will be used to investigate the dissemination of the tungro virus within rice plants, incorporating two distinct strategies for its control. These treatments encompass managing plants through the removal of infected ones and managing the vector responsible for spreading the tungro virus by employing insecticides. The population of rice plants will be categorized into three distinct subgroups: one comprising susceptible plants denoted as S_h, the other comprising plants infected with the tungro virus denoted as I_h, and a third comprising virus-resistant rice plants denoted as R_h. At the same time, the population of planthoppers,

acting as carriers of the tungro virus, is segregated into two subgroups: one susceptible subgroup labeled as S_v and another consisting of infected planthoppers denoted as I_v. A visual representation of the interplay between these two populations is presented in Figure 1.

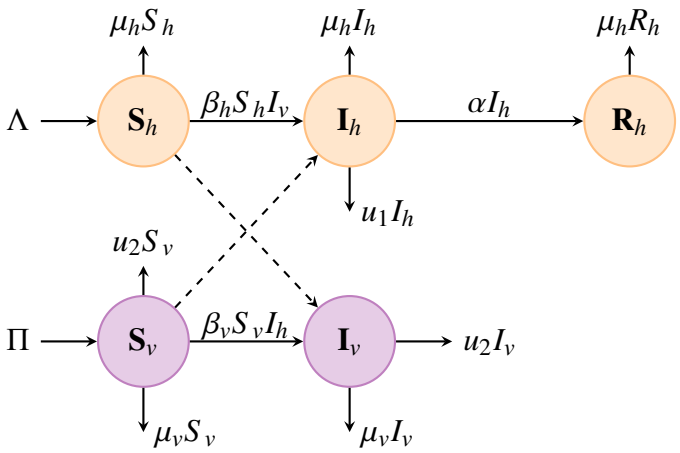

FIGURE 1. Diagram illustrating the interaction between sub-populations of rice plants, categorized into three groups, and populations of planthoppers responsible for transmitting the Tungro virus.

Each sub-group within the rice plant or planthopper pest populations experiences a natural mortality rate, denoted as μ_h and μ_v respectively. When a subpopulation of uninfected rice plants encounters infected planthoppers, a portion of these uninfected plants transitions into the infected rice compartment, occurring at a rate of β_h. Nevertheless, some rice plants that have interacted with infected planthoppers do not display any symptoms and are thus classified as resistant. In contrast to human populations, where individuals can be classified as resistant post-vaccination, determining resistance in rice plant populations relies on their interaction with planthoppers carrying the tungro virus without exhibiting infection symptoms. Consequently, there exists a rate (α) at which rice plants transition from the infected subpopulation to the resistant subpopulation. It's important to clarify that in this scenario, we are assuming that the subpopulation of resistant rice plants does not serve as a vector for transmitting the tungro virus through the leafhopper population. Conversely, when a healthy planthopper subpopulation interacts with an infected rice subpopulation, the healthy planthopper individuals shift to the infected planthopper population at a rate of β_v.

To manage the tungro virus's spread, infected rice plant subpopulations were reduced by a rate of u_1 through cutting. Simultaneously, in order to decrease the planthopper pest population, insecticides are employed, causing a mortality rate of u_2 among the planthopper pests. Equation 2.1 presents the comprehensive dynamic model that outlines the propagation of the tungro virus, taking into account these two interventions. Briefly, we have compiled a summary of parameter descriptions, including both standard values and value ranges, for the parameters used in equation 2.1, presented in Table 1.

$$
\begin{aligned}
\frac{dS_h}{dt} &= \Lambda - \beta_h S_h I_v - \mu_h S_h \\
\frac{dI_h}{dt} &= \beta_h S_h I_v - (u_1 + \alpha + \mu_h) I_h \\
\frac{dR_h}{dt} &= \alpha I_h - \mu_h R_h \\
\frac{dS_v}{dt} &= \Pi - \beta_v S_v I_h - (u_2 + \mu_v) S_v \\
\frac{dI_v}{dt} &= \beta_v S_v I_h - (u_2 + \mu_v) I_v
\end{aligned}
\tag{2.1}
$$

TABLE 1. Description of the parameters and their value.

Par	Description	Standard Value	Range	unit	Ref
Λ	recruitment rate of plant	8	0 –10	$plant \cdot daya^{-1}$	[37]
β_h	infection rate due to interaction with infected planthopper	0.008	0.002–0.032	$vector^{-1} day^{-1}$	[38]
μ_h	natural date rate of plant populations	0.003	0–0.033	day^{-1}	[38]
u_1	control of plant by pruning intervention		0 – 1	day^{-1}	assumed
α	the proportion of plants that are resistant to the virus	0.003	0 – 1	day^{-1}	assumed
Π	recruitment rate of planthopper population	10	0 – 10	$vector \cdot day^{-1}$	[37]
β_v	infection rate due to interaction with infected plant	0.008	0.002–0.032	day^{-1}	[38]
u_2	control of planthopper populations with insecticide interventions	0.3	0 – 1	day^{-1}	[37]
μ_v	natural death rate of planthopper populations	0.12	0.06–0.18	day^{-1}	[38]

It should be emphasized that the model presented in system (2.1) is augmented with initial conditions that ensure non-negativity, as outlined below.

$$S_h(0) \geq 0, \qquad I_h(0) \geq 0, \qquad R_h(0) \geq 0, \qquad S_v(0) \geq 0, \qquad I_v(0) \geq 0.$$

All parameters are presumed to maintain constant values and remain non-negative throughout. Employing the aforementioned initial conditions, the positivity of the solution to the system (2.1) can be achieved, as will be demonstrated shortly in the subsequent section of our analysis.

Nevertheless, it is important to acknowledge that this particular model is encumbered by a multitude of inherent limitations, one of the most significant being the presumption that all parameters remain constant and unchanging throughout the passage of time, a notion that may not accurately encapsulate the intricate biological and environmental dynamics that are typically observed in the field of study. Additionally, the model's neglect of the numerous environmental influences, including but not limited to climate fluctuations and the intricate interrelationships between diverse plant populations and other pest species, is a critical oversight. These elements have been demonstrated to exert a substantial influence on the transmission and proliferation of the Tungro virus.

3. Mathematical Analysis

3.1. Invariant and Bounded Solution. Prior to undertaking further analysis, it is essential to ascertain that the system of non-linear differential equations presented in equation (2.1) is both mathematically well-posed and biologically realistic. To this end, it is necessary to demonstrate the existence of a positively invariant set and the bounded solution. To prove that the solution of a system of differential equations is an invariant set, we need to show that if the initial values of the solution start from the first octant, then the solution will never leave the first octant over time, even as $t \to \infty$. Assume the initial value of the system is in the first octane, i.e. $S_h(0) \geq 0, I_h(0) \geq 0, R_h(0) \geq 0, S_v(0) \geq 0,$ and $I_v(0) \geq 0$. The first octant in this context is a subset of 5-dimensional space where all coordinate components are nonnegative. To ensure that the solution remains within the first octant, we consider the behavior of the system at the boundaries of the octant space. Here, the external normal vectors $\mathbf{n}$ at the octant boundaries are used to analyze the direction of the vector fields of the system of differential equations. If we

compute the dot product between the vector field of system (2.1) and the external normal vector **n** evaluated at the octant boundary, we find that the result is always nonpositive. This means that the vector field forms an obtuse or perpendicular angle to the external normal vector, indicating that the direction of the vector field tends to enter the octant or remain at the boundary. The implication of this analysis is that the solution to the system cannot leave the first octant because the vector field pushes the solution back into the octant or remains on the octant boundary. Thus, it can be concluded that the solution to this system of differential equations is permanently confined within the first octant in 5-dimensional space.

Further to show the bounded solution, let us assume that $P(t) = S_h(t) + I_h(t) + R_h(t)$ and $A(t) = S_v(t) + I_v(t)$. From equation 2.1, it can be demonstrated that

$$\begin{aligned}\frac{dP}{dt} &= \frac{dS_h}{dt} + \frac{dI_h}{dt} + \frac{dR_h}{dt} \\ &= \Lambda - \mu_h(S_h + I_h + R_h) - u_1 I_h\end{aligned}$$

If we exclude the mortality proportion resulting from cutting a specific quantity of infected plants ($u_1 = 0$), the resulting equation can be simplified to:

$$\frac{dP}{dt} + \mu_h P \leq \Lambda$$

The integration of the two sides yields the following result:

$$\begin{aligned}P(t)e^{\mu_h t} &\leq \int \Lambda e^{\mu_h t} dt + C \\ &= \frac{\Lambda}{\mu_h} e^{\mu_h t} + C \\ P(t) &\leq \frac{\Lambda}{\mu_h} + Ce^{-\mu_h t}\end{aligned}$$

where C is a constant. By employing the initial value $P(0) = P_0$, we derive the result $C = P_0 - \frac{\Lambda}{\mu_h}$, which implies that

$$P(t) \leq \frac{\Lambda}{\mu_h}(1 - e^{-\mu_h t}) + P_0 e^{-\mu_h t} \tag{3.1}$$

From the equation (3.1) it can be seen that for $t \to \infty$ then $P(t) \to \frac{\Lambda}{\mu_h}$. This show that the system of $\frac{dP}{dt}$ is bounded. In the same way it can also be seen that $\frac{dA}{dt}$ has bounded solutions.

3.2. Basic Reproduction Number and DFE Stability. Under conditions of equilibrium, the DFE (Disease-Free Equilibrium) is attained by solving the system of equation (2.1) in the absence of infected quantities, yielding the following result:

$$DFE := \left\{ S_h = \frac{\Lambda}{\mu_h}, I_h = 0, R_h = 0, S_v = \frac{\Pi}{u_2 + \mu_v}, I_v = 0 \right\} \tag{3.2}$$

The Jacobian matrix of system (2.1) evaluated at any point $X = (S_h, I_h, R_h, S_v, I_v)$ is

$$J(X) = \begin{pmatrix} -\beta_h I_v - \mu_h & 0 & 0 & 0 & -\beta_h S_h \\ \beta_h I_v & -u_1 - \alpha - \mu_h & 0 & 0 & \beta_h S_h \\ 0 & \alpha & -\mu_h & 0 & 0 \\ 0 & 0 & 0 & -I_v \beta_v - \mu_v - u_2 & -\beta_v S_v \\ 0 & \beta_v S_v & 0 & \beta_v I_h & -\mu_v - u_2 \end{pmatrix} \tag{3.3}$$

As a generally accepted concept, the basic reproduction number is determined when there is one infected individual within a population where all individuals have the potential to become infected [39]. Various methods for calculating the basic reproduction number expression are available, some of which are outlined in references [39, 40], and these methods are also employed in our work. The Jacobian matrix of system (2.1) is computed at equilibrium point (3.2) under the Disease-Free Equilibrium (DFE) condition. Subsequently, this matrix is divided into a transition matrix and a transmission matrix to ascertain the spectral radius of the matrix $\rho(\mathscr{F}\mathscr{V}^{-1})$, in the following context:

$$\mathscr{F} = \begin{pmatrix} 0 & \frac{\beta_h \Lambda}{\mu_h} \\ \frac{\beta_v \Pi}{\mu_v + u_2} & 0 \end{pmatrix}, \quad \text{and} \quad \mathscr{V}^{-1} = \begin{pmatrix} -(u_1 + \alpha + \mu_h)^{-1} & 0 \\ 0 & -(\mu_v + u_2)^{-1} \end{pmatrix}.$$

As a result, the expression for $\mathscr{R}_0$ is derived as follows :

$$\mathscr{R}_0 := \frac{\beta_h \beta_v \Lambda \Pi}{(u_2 + \mu_v)^2 (u_1 + \alpha + \mu_h) \mu_h}. \tag{3.4}$$

By examining the DFE equilibrium expression in equation (3.2), it becomes apparent that the presence of this equilibrium is independent of the value of $\mathscr{R}_0$. This indicates that the DFE equilibrium will persist under all circumstances, regardless of the magnitude of $\mathscr{R}_0$.

We will now examine the local stability of the Disease-Free Equilibrium (DFE) by assessing the Jacobian matrix of system (2.1) at the DFE. We can explicitly determine the three eigenvalues of the Jacobian matrix as follows: $\lambda_1 = -\mu_h$ with a multiplicity of two, and $\lambda_2 = -(u_2 + \mu_v)$. The signs of the remaining two eigenvalues can be inferred from the polynomial equation (3.5).

$$p_1(\lambda) := \lambda^2 + \underbrace{(\mu_v + \alpha + \mu_h + u_1 + u_2)}_{:=A_1}\lambda \underbrace{-(\mu_v + u_2)(u_1 + \alpha + \mu_h)(\mathscr{R}_0 - 1)}_{:=A_0} \tag{3.5}$$

We observe that the coefficient A_1 in polynomial (3.5) consistently exhibits a positive value, thereby indicating that the stability of the Disease-Free Equilibrium (DFE) is contingent upon the constant term A_0 within the polynomial. It becomes evident that the constant A_0 assumes a positive value when $\mathscr{R}_0 < 1$. This signifies that the DFE equilibrium is stable when the condition $\mathscr{R}_0 < 1$ is met. Conversely, if $\mathscr{R}_0 > 1$, the constant A_0 assumes a negative value, signifying the instability of the DFE equilibrium, as one of the eigenvalues in (3.5) becomes positive.

3.3. Endemic Equilibrium and its Stability. Upon eliminating I_v from equation (2.1) while considering equilibrium conditions, we derive the endemic equilibrium point (END), which is contingent upon the compartment I_v, as described below.

(3.6)

$$END := \left\{ S_h^* = \frac{\Lambda}{\beta_h I_v^* + \mu_h}, I_h^* = \frac{I_v^*(u_2 + \mu_v)\left(\beta_v I_v^* + u_2 + \mu_v\right)}{\Pi\beta_v}, R_h^* = \frac{\alpha}{\mu_h} I_h^*, S_v^* = \frac{\Pi}{\beta_v I_v^* + u_2 + \mu_v} \right\}$$

where I_v^* is the root of the following polynomial equation (3.7).

$$p_2(I_v) = \beta_h\beta_v I_v^2 + \left(\beta_h(u_2 + \mu_v) + \beta_v\mu_h\right) I_v - \mu_h(u_2 + \mu_v)(\mathscr{R}_0 - 1) \tag{3.7}$$

Looking at the polynomial (3.7), it becomes apparent that a sole positive root for the polynomial I_v^* emerges when $\mathscr{R}_0 > 1$ This indicates that the existence of an endemic equilibrium is assured under the condition of $\mathscr{R}_0 > 1$, whereas there is no endemic equilibrium when $\mathscr{R}_0 < 1$.

The Monte Carlo simulation approach is used to prove the stability of the equilibrium point in the $\mathscr{R}_0 > 1$ region, as explained in the article by [41]. The parameters required in this analysis are summarized in Table 1, where the values of u_1 and u_2 are randomly generated based on a uniform distribution. During the simulation, the generated parameters are filtered so that only values that satisfy the internal equilibrium stability conditions are used for further analysis. The

results of the Monte Carlo simulation are visualized in Figure 2, which provides an overview of the stability of the system in the region studied.

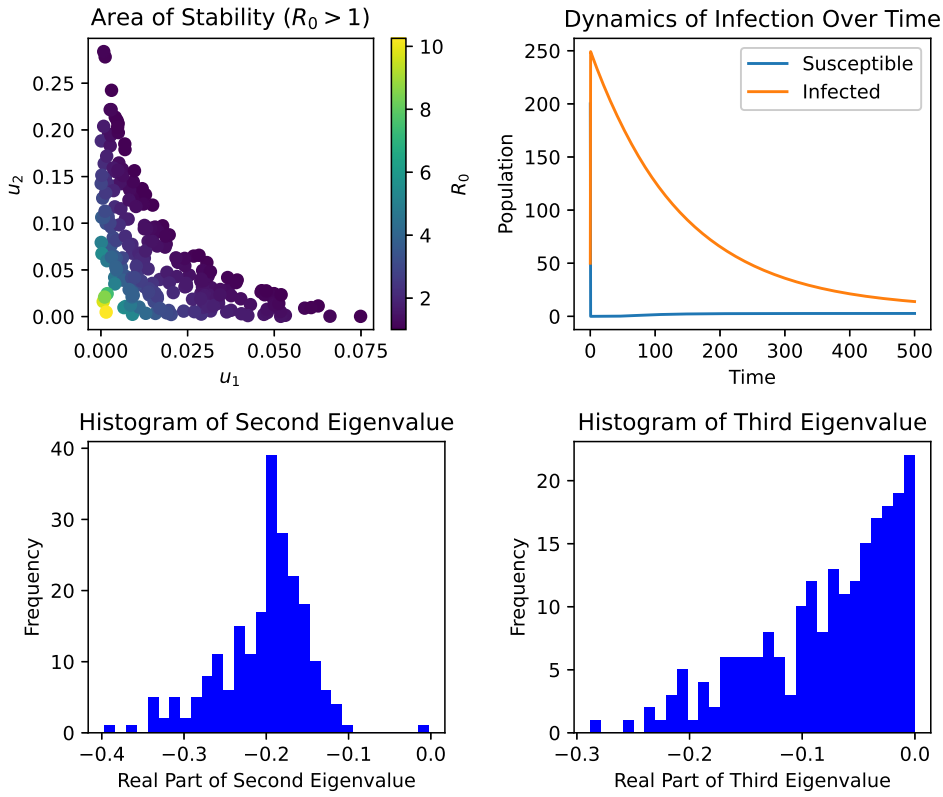

FIGURE 2. Stability of the $\mathscr{R}_0 > 1$ region with the Monte Carlo method approach

The first image in Figure 2 shows the random values u_1 and u_2, which are in the interior of the equilibrium stability region. On the other hand, the second image shows the dynamics of the system, specifically in the susceptible and infected rice compartments. This system produces five eigenvalues, three of which are independent of the parameters u_1 and u_2 and all have negative signs. The distribution of the other two eigenvalues, which depend on the parameters u_1 and u_2, is shown in the second row of Figure 2. From the visualization, it can be seen that the distribution of the two eigenvalues is entirely in the negative region. This indicates that the internal equilibrium is stable in the region $\mathscr{R}_0 > 1$.

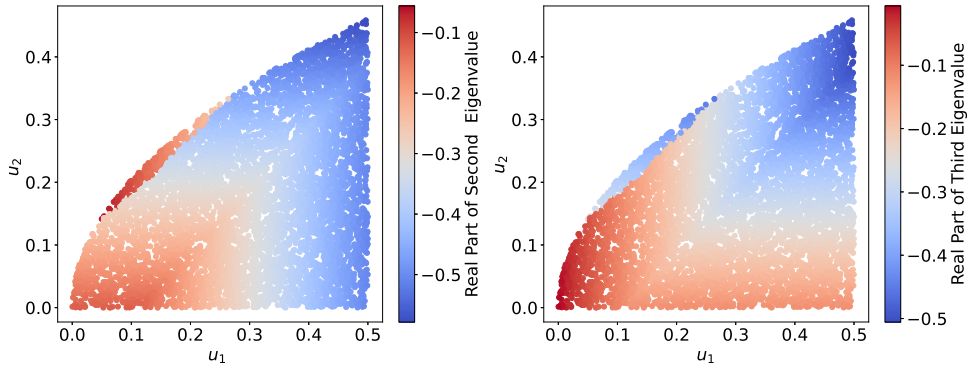

FIGURE 3. Robustness Analysis: Effect of Parameters on Stability

Figure 3 shows the robustness analysis of the effect of variation of parameters u_1 and u_2 on the sign of the eigenvalues as an indicator of system stability. The left figure shows the distribution of the real part of the second eigenvalue on the parameters u_1 and u_2. Meanwhile, the right figure shows the distribution of the real part of the third eigenvalue. The color in each panel indicates the sign of the eigenvalue, with red indicating values closer to zero and blue indicating more negative values. This distribution confirms that changes in parameters u_1 and u_2 consistently produce eigenvalues that remain in the negative region, especially in the region of system stability. Thus, this analysis proves that the system maintains interior equilibrium stability over the entire range of parameter values u_1 and u_2, indicating the robustness of the system stability to parameter variations.

4. Numerical Simulation and Biological Interpretation

4.1. Qualitative Behaviour. The simulation of the solution of model (2.1) without controls ($u_1 = u_2 = 0$) versus time is given in Figure 4. We use parameter values as in Table 1 but with $\Lambda = \Pi = 0.1$ and the following initial condition $(S_h, I_h, R_h, S_v, I_v) = (200, 50, 0, 50, 10)$. By these parameter values, we have the basic reproduction number $\mathscr{R}_0 = 2.46$, so in this case, the simulation will produce an endemic. We differentiate the simulation for the case of plant population and planthopper population. As illustrated in Figure 4a, the observed population of healthy plants, denoted as S_h, experiences a marked decline in numbers at the onset of the interaction. This decline can be attributed to the detrimental effects stemming from interactions with infected planthoppers. Conversely, the population of infected plants (I_h), exhibits a rapid increase

initially, followed by a gradual decline as the system approaches a state of equilibrium. Furthermore, the population of recovered plants (R_h), experiences an initial surge due to the acquisition of resistance mechanisms, yet it ultimately stabilizes at a particular value, which is constrained by limitations in available resources. In Figure 4b, the population of healthy planthoppers (S_v), undergoes a gradual decline due to the propagation of infection by infected plants. In contrast, the population of infected planthoppers (I_v), experiences a brief period of increase before reaching a state of stabilization. These observable trends serve to elucidate the direct ramifications of infection on both plant populations and their corresponding vectors, culminating in the attainment of equilibrium when the interactions between the various populations cease to contribute to the escalation of infection rates.

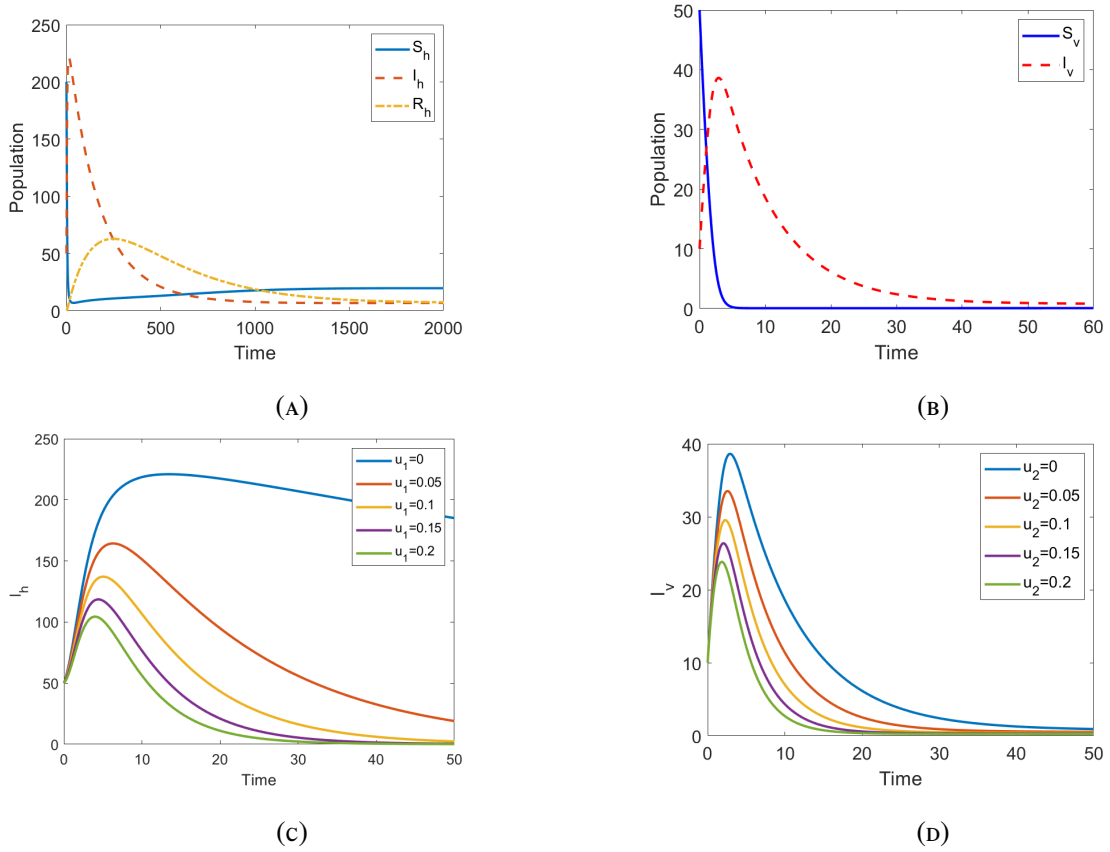

FIGURE 4. Solution of (a) plant's compartments S_h, I_h, R_h, and (b) virus's compartments S_v, I_v. The behaviour of (c) infected plant as control u_1 vary, and (d) infected virus as control u_2 vary.

The objective of control of plant by pruning intervention, denoted by u_1, is to remove the infected plants so that the virus transmission can be minimized. From the previous simulation we show that even without control u_1 the infected plant population decreases in a long time. But, in Figure 4c, the presence of control u_1 makes the infected plant population decreases more rapidly, moreover at certain value of u_1 the infected plant population can become extinct. On the other hand, the implementation of u_2 control, which involves the strategic application of insecticides meticulously designed to mitigate the population density of leafhoppers, has resulted in a significant decrease in the number of infected leafhoppers, as illustrated in Figure 4d. This outcome is of considerable importance because it curtails the potential dissemination of viral pathogens to other plant species within the ecosystem. However, it is noteworthy that the populations of healthy leafhoppers may persist in the environment despite these efforts.

4.2. Sensitivity Analysis.

4.2.1. *Elasticity Index.* The basic reproduction number, denoted $\mathscr{R}_0$, is the estimated number of cases where plants and planthoppers are vulnerable to infection that would be directly created by one case. In Eq. (3.4), the value of $\mathscr{R}_0$ is influenced by parameters β_h, β_v, Λ, Π, α, μ_h, μ_v, and controls u_1, u_2. In the previous section, it has been demonstrated that if $\mathscr{R}_0 < 1$ then the diseases is free, and on the other hand, if $\mathscr{R}_0 > 1$ the disease becomes endemic. Thus, those parameters affect directly to the beginning of the disease transmission. But, which one will have most impact on the disease transmission? This question can be answered through studying the elasticity index of the basic reproduction number.

The elasticity index of $\mathscr{R}_0$ of parameter p is calculated by

$$\Upsilon_p^{\mathscr{R}_0} = \frac{\partial \mathscr{R}_0}{\partial p} \times \frac{p}{\mathscr{R}_0}, \tag{4.1}$$

where $p \in \{\beta_h, \beta_v, \Lambda, \Pi, \alpha, \mu_h, \mu_v, u_1, u_2\}$. The elasticity index gives a normalized sensitivity of $\mathscr{R}_0$. Thus, the parameter that has biggest absolute value of the elasticity index will be interpreted as the best parameter to be controlled in order to curb the disease transmission.

We provide the calculation of the elasticity index as a chart in Figure 5. It can be observed that the control u_2 is the most sensitive aspect in the disease transmission. Therefore, the insecticide intervention will be the most effective way to control the disease transmission. The second most

sensitive parameter is μ_h. We may interpret it as follows. The plant with superior varieties, especially for low natural death rate, will be less suffered from the disease and lower the disease transmission. The less sensitive parameter is α. This means that the proportional of resistance plant provide less contribution to the disease transmission.

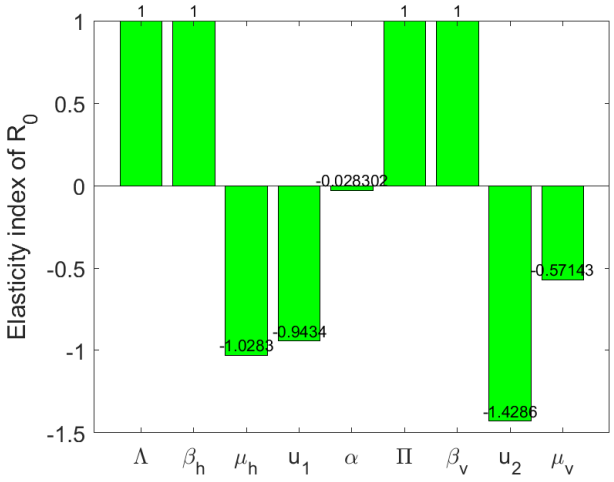

FIGURE 5. Elasticity index of $\mathscr{R}_0$.

4.2.2. *Contour of the Basic Reproduction Number.* Suppose that $\mathscr{R}_0$ in (3.4) is seen as a function of two parameters. It is interesting to perform a sensitivity analysis by observing the contour plot of $\mathscr{R}_0$. From this point of view, we can observe the simultaneous impact from a combination of two parameters. For the simulation purposes, there are three cases: a combination of parameters for each plant and planthopper models, a combination of parameters with interplay effect between plant and planthopper, and a combination of infection rates with controls. In Figure 6, we present the contour plot of $\mathscr{R}_0$ as a function of two parameters for plant model: (β_h, Λ), (β_h, μ_h), (β_h, α), and for planthopper model: (β_v, Π), (β_v, μ_v). For the case of (β_h, Λ) and (β_v, Π), they have similar effects on $\mathscr{R}_0$, that is the greater their value the more rapid the disease transmission. Meanwhile, the case of (β_h, μ_h), (β_h, α), and (β_v, μ_v), the greater the value of infection rates and the less the value of α, μ_h, and μ_v, the more rapid the disease transmission.

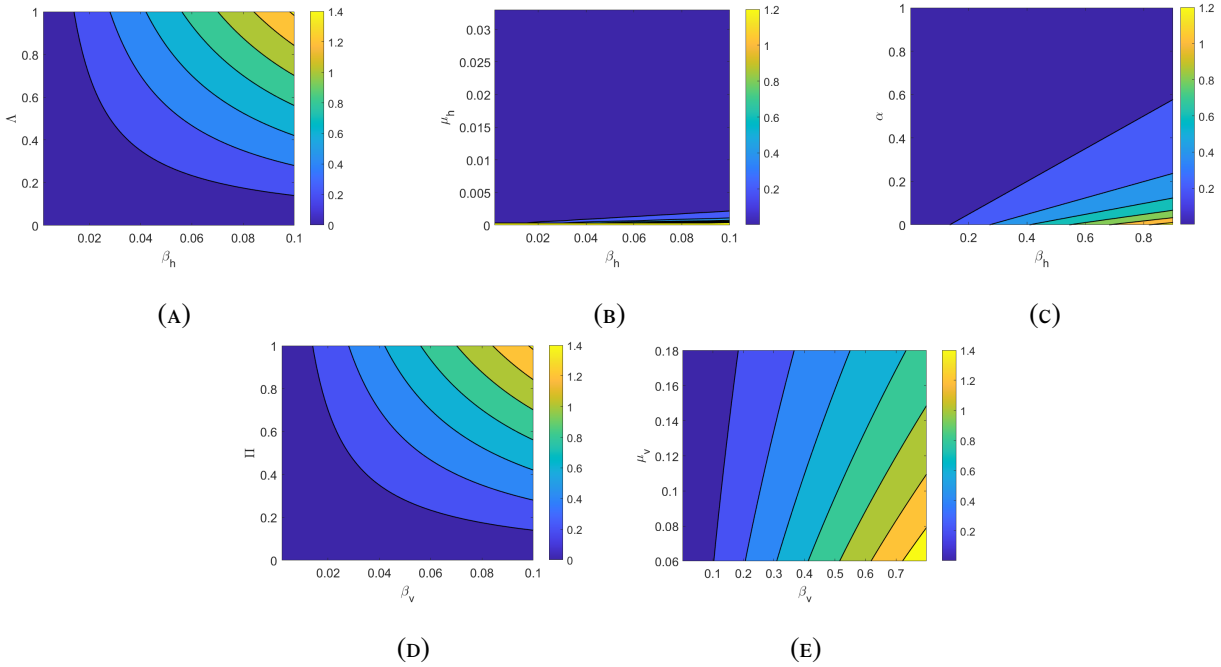

(A) (B) (C)

(D) (E)

FIGURE 6. Contour plot of $\mathscr{R}_0$ as a function of (a-c) combination of plant's parameters β_h with Λ, α, μ_h, and (d-e) combination of virus's parameters β_v with Π, μ_v.

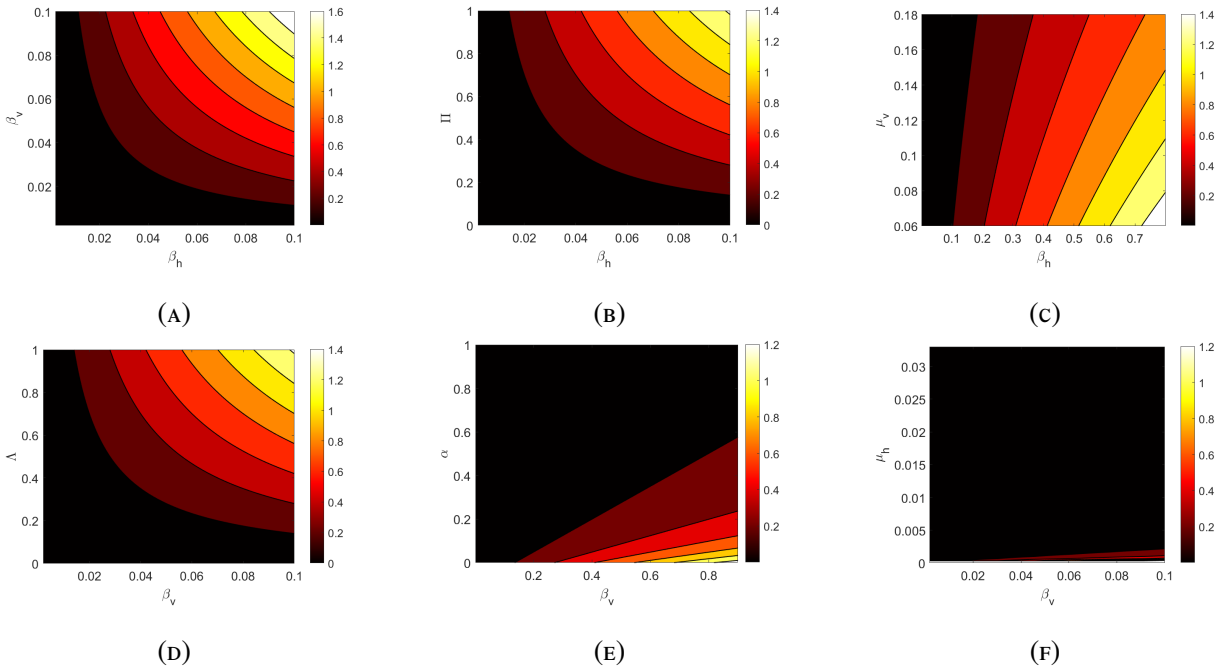

(A) (B) (C)

(D) (E) (F)

FIGURE 7. Contour plot of $\mathscr{R}_0$ as a function of (a-c) combination of β_h with virus's parameters β_v, Π, μ_v, and (d-e) combination of β_v with plant's parameters Λ, α, μ_h.

Figure 7 presents a contour plot analysis of the basic reproduction number ($\mathscr{R}_0$) in response to variations in key model parameters. This sensitivity analysis reveals how $\mathscr{R}_0$ is influenced by interactions between different biological and epidemiological factors related to both the plant and planthopper populations. Subplot (A) illustrates that increasing both the infection rate due to interaction with infected planthopper (β_h) and the infection rate due to interaction with infected plant (β_v) leads to a significant increase in $\mathscr{R}_0$. This indicates that the bidirectional transmission cycle between plants and planthoppers plays a critical role in sustaining virus spread. In subplot (B), a similar increasing trend is observed when β_h is combined with the recruitment rate of planthopper population (Π), suggesting that a larger vector population amplifies the potential for plant infection. Subplot (C) shows that higher values of the natural death rate of planthopper populations (μ_v) result in a noticeable decrease in $\mathscr{R}_0$, even when β_h remains high. This implies that vector mortality is a crucial factor in suppressing disease transmission. Subplot (D) highlights the positive relationship between β_v and the plant recruitment rate (Λ), emphasizing that an increased availability of host plants contributes to the persistence and expansion of the virus. In subplot (E), $\mathscr{R}_0$ increases with higher values of the infection rate β_v, especially when the proportion of virus-resistant plants (α) is low. However, as α increases, the value of $\mathscr{R}_0$ decreases, demonstrating the protective effect of resistance within the plant population. Lastly, subplot (F) illustrates that increasing the natural death rate of plant populations (μ_h) corresponds with a reduction in $\mathscr{R}_0$, indicating that a shorter lifespan of susceptible plants can help disrupt the transmission chain. Overall, the results indicate that transmission-related parameters (β_h, β_v), population recruitment rates (Π, Λ), and the proportion of resistant plants (α) are positively associated with increases in $\mathscr{R}_0$. In contrast, natural mortality rates of both vectors and hosts (μ_v, μ_h) are inversely related to $\mathscr{R}_0$, suggesting that vector control and plant resistance are key strategies for mitigating the spread of the disease.

Figure 8 further explores the impact of control strategies on $\mathscr{R}_0$. Subplot (A) shows that increasing the control parameter u_1, representing pruning intervention on infected plants, significantly reduces $\mathscr{R}_0$, even under high values of β_h. The gradient from red to blue indicates the strong efficacy of this control measure. Subplot (B) depicts the effect of insecticidal control (u_2) on the planthopper population, in relation to the infection rate from plants (β_v). As u_2 increases,

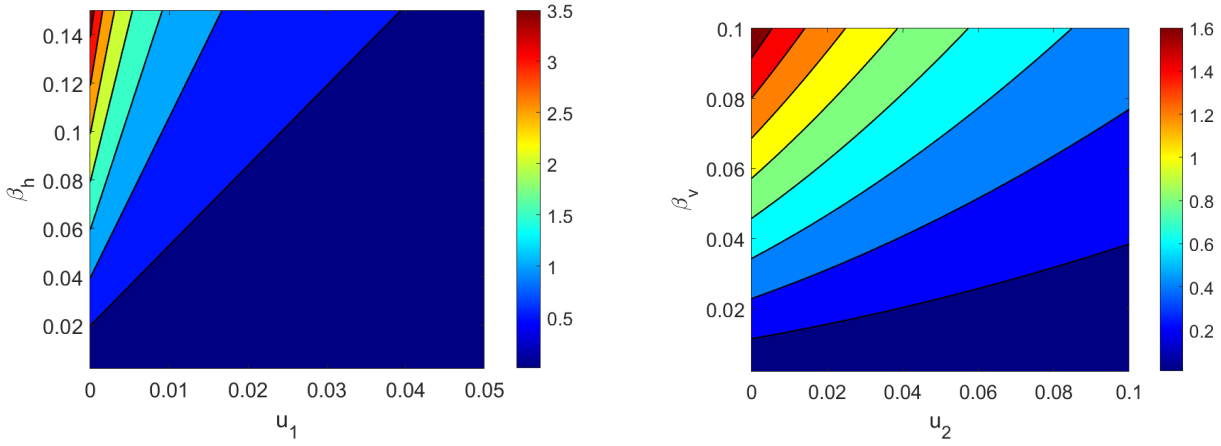

(A) (B)

FIGURE 8. Contour plot of $\mathscr{R}_0$ as a function of (a) control u_1 with β_h, and (b) control u_2 with β_2.

$\mathscr{R}_0$ decreases substantially, especially when β_v is high, emphasizing the role of vector control in managing disease spread. Together, these results highlight that both plant-based control (u_1) and vector-based control (u_2) are effective in reducing the reproduction number, suggesting that an integrated management strategy would be most effective in controlling the epidemic.

4.2.3. *Time-dependent sensitivity of parameters.* Suppose a vector of variables $X = (S_h, I_h, R_h, S_v, I_v)$, a vector of parameters $P = (\Lambda, \beta_h, \mu_h, u_1, \alpha, \Pi, \beta_v, u_2, \mu_v)$, and a vector of the right-hand side of (2.1) F. Define $S = \frac{\partial X}{\partial P}$. By total differential, we have

$$\frac{dS}{dt} = J(X)S + \frac{\partial F}{\partial P}, \tag{4.2}$$

where $J(X)$ is the 5×5 Jacobian matrix (3.3), S and $\frac{\partial F}{\partial P}$ are 5×9 matrix, where

$$S = \begin{bmatrix} \frac{\partial S_h}{\partial \Lambda} & \frac{\partial S_h}{\partial \beta_h} & \cdots & \frac{\partial S_h}{\partial \mu_v} \\ \frac{\partial I_h}{\partial \Lambda} & \frac{\partial I_h}{\partial \beta_h} & \cdots & \frac{\partial I_h}{\partial \mu_v} \\ \vdots & \vdots & \ddots & \vdots \\ \frac{\partial I_v}{\partial \Lambda} & \frac{\partial I_v}{\partial \beta_h} & \cdots & \frac{\partial I_v}{\partial \mu_v} \end{bmatrix} \tag{4.3}$$

and

$$\frac{\partial F}{\partial P} = \begin{bmatrix} 1 & -S_h I_v & -S_h & 0 & 0 & 0 & 0 & 0 & 0 \\ 0 & S_h I_v & -I_h & -I_h & -I_h & 0 & 0 & 0 & 0 \\ 0 & 0 & -R_h & 0 & I_h & 0 & 0 & 0 & 0 \\ 0 & 0 & 0 & 0 & 0 & 1 & -S_v I_h & -S_v & -S_v \\ 0 & 0 & 0 & 0 & 0 & 0 & S_v I_h & -I_v & -I_v \end{bmatrix} \tag{4.4}$$

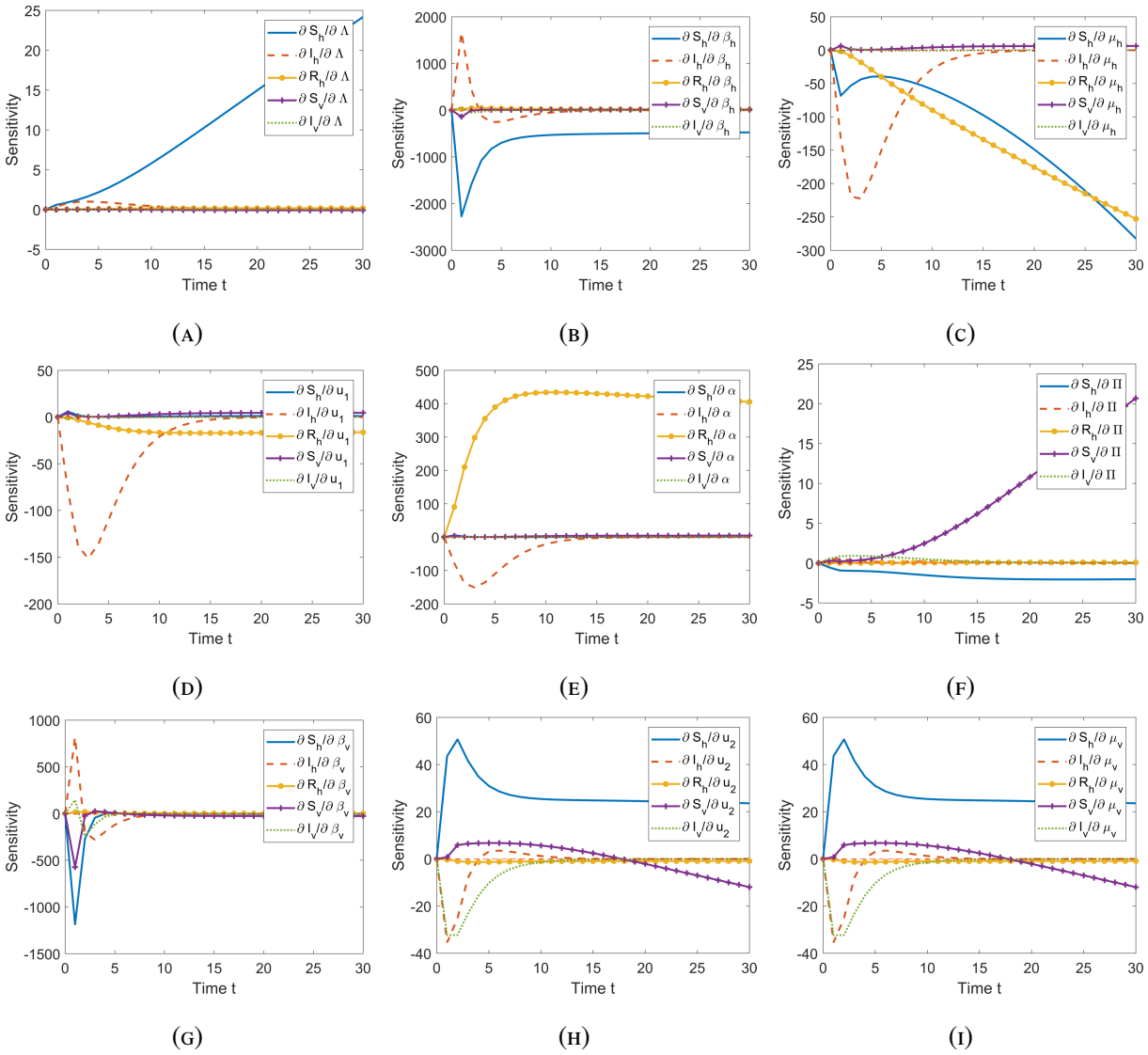

FIGURE 9. Time-dependent sensitivity of parameters.

Figure 9 depicts a numerical solution of equation (4.2), illustrating the evolving sensitivity levels of all parameters to all variables over time. Over time, parameter Λ exhibits high sensitivity to the population of healthy rice plants, denoted as S_h (refer to figure 9a). This indicates that even a slight rise in the value of Λ significantly influences the increase in population of S_h. Meanwhile, parameter β_h demonstrates a pronounced sensitivity to the negative impact on variable S_h as time progresses (refer to Figure 9b). The significant impact on the abundance of healthy rice populations stems from the minute increments in parameter β_h, resulting in a reduction in the healthy rice plant population. Conversely, minimizing the infection rate leads to an increase in healthy rice plant populations. These findings elucidate the potential to diminish the population of infected plants through mitigation of the infection rate. Strategies encompassed within the model for reducing the infection rate include pruning and the application of insecticides. In Figure 9c, it becomes evident that during the initial phase, parameter μ_h is responsive to fluctuations in variable I_h; however, as equilibrium conditions are reached, particularly at $t = 30$, the natural death rate parameter becomes influential. This suggests that the regulation of plant infection via natural death rates holds significance primarily during the proximity to initial conditions. However, as equilibrium is approached, its effect becomes more pronounced in diminishing the population of healthy plants compared to infected ones.

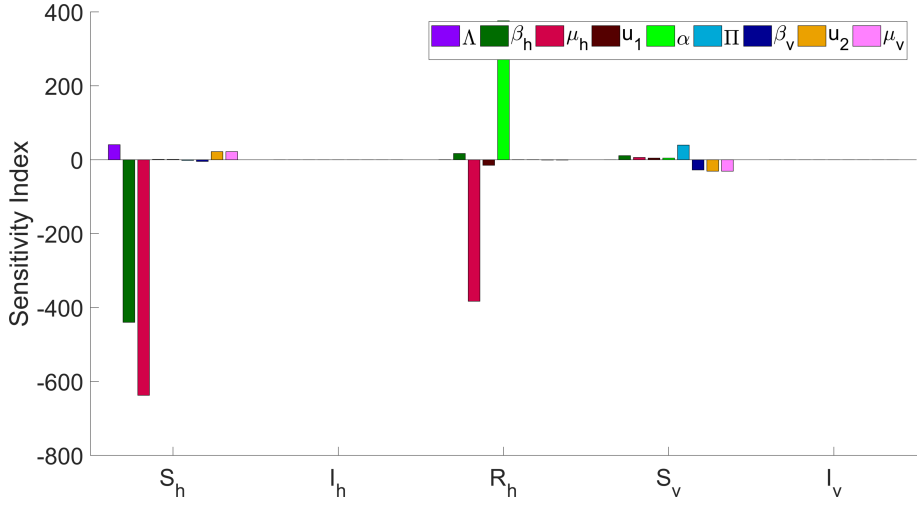

FIGURE 10. Sensitivity index of parameters after reaching $t = 50$.

4.3. Optimal Scenario Simulation. From previous analysis, we can see that increasing u_1 and/or u_2 can successfully reduce $\mathcal{R}_0$. However, high intensity of these intervention resulting

in a high cost of intervention. The intervention should be adapted with the current condition at each time. Hence, control parameter should be depend on time t. Our aim is to minimize the number of infected individuals I_h and I_v with as low as possible rate of intervention u_1 and u_2. This aims reflected in the following cost function.

$$\mathcal{J} = \int_0^T \left(\varepsilon_1 I_h + \varepsilon_2 I_v + \frac{c_1}{2}u_1^2 + \frac{c_2}{2}u_2^2\right)dt, \tag{4.5}$$

where ε_1 and ε_2 is the weight parameter for infected compartment, while c_1 and c_2 for control variables u_1 and u_2, respectively.

To characterize the optimal control problem, lets define the Hamiltonian function of our problem as follows:

$$\mathcal{H} = \varepsilon_1 I_h + \varepsilon_2 I_v + \frac{c_1}{2}u_1^2 + \frac{c_2}{2}u_2^2 + \lambda_1\frac{dS_h}{dt} + \lambda_2\frac{dI_h}{dt} + \lambda_3\frac{dR_h}{dt} + \lambda_4\frac{dS_v}{dt} + \lambda_5\frac{dI_v}{dt} \tag{4.6}$$

On the other hand, taking the negative partial derivative of $\mathcal{H}$ with respect to each state variables, we obtain:

$$\frac{d\lambda_1}{dt} = (I_v\beta_h + \mu_h)\lambda_1 - \lambda_2\beta_h I_v \tag{4.7}$$

$$\frac{d\lambda_2}{dt} = -\varepsilon_1 + (u_1 + \alpha + \mu_h)\lambda_2 - \alpha\lambda_3 + \lambda_4\beta_v S_v - \lambda_5\beta_v S_v \tag{4.8}$$

$$\frac{d\lambda_3}{dt} = \lambda_3\mu_h \tag{4.9}$$

$$\frac{d\lambda_4}{dt} = (\beta_v I_h + \mu_v + u_2)\lambda_4 - \beta_v I_h\lambda_5 \tag{4.10}$$

$$\frac{d\lambda_5}{dt} = -\varepsilon_2 + \beta_h S_h\lambda_1 - \beta_h S_h\lambda_2 + (u_2 + \mu_v)\lambda_5 \tag{4.11}$$

where the transversality condition $\lambda_i(T_f) = 0$ for $i = 1..5$. The optimal control variables for tree pruning intervention u_1 is obtained by solving $\dfrac{d\mathcal{H}}{du_1} = 0$ respect to u_1, which gives us $u_1^* = \dfrac{I_h\lambda_2}{c_1}$. Considering budget constraints and preferences, we establish a lower bound $u_1^{\min}$ and an upper bound $u_1^{\max}$ for u_1. Consequently, the optimal solution for the tree pruning intervention is represented by equation (4.12).

$$u_1^\dagger = \max\left\{u_1^{\min}, \min\left\{u_1^{\max}, \frac{I_h\lambda_2}{c_1}\right\}\right\}. \tag{4.12}$$

Using a similar method, we can also determine the optimal solution for implementing insecticide intervention u_2 given by equation (4.13).

$$u_2^{\dagger} = \max\left\{u_1^{\min}, \min\left\{u_1^{\max}, \frac{S_v\lambda_4 + I_v\lambda_5}{c_2}\right\}\right\}. \tag{4.13}$$

Furthermore, We perform numerical experiment for this optimal control problem. To run the simulation, we use parameter values as given in Table 1 and the following initial condition $(S_h, I_h, R_h, S_v, I_v) = (200, 50, 0, 50, 10)$. We use forward-backward sweep method to solve our problem. Please see [42] for further explanation and example. We conduct the simulation in three different strategy i.e. combination of u_1 and u_2, implementation of u_1 only, implementation of u_2 only.

Scenario 1. The first simulation is conducted to assess the impact of the combination of u_1 and u_2 in reducing the spread of diseases. The results are presented in Figure 11. Panels (f) and (g) depict the dynamics of u_1 and u_2.We can observe that a high intensity of u_1 and u_2 should be applied from the beginning of the simulation and gradually decreased as we approach the final time of the simulation. The maximum values of u_1 and u_2 are 0.246 and 0.64, respectively. As a result of the high intensity of u_1, we can see a reduction in the number of infected individuals (I_h) in panel (b) and an increase in the number of susceptible individuals (S_h) and individuals who have recovered (R_h) in panels (a) and (c), respectively. A high intensity of u_2 results in a reduced number of susceptible and infected vectors (please refer to panels (d) and (e)). In this scenario, the cost function $\mathcal{J}$ is 62.334.

Scenario 2. The next simulation is aimed at understanding the potential of u_1 in reducing the spread of disease when u_1 is implemented as the single-intervention. The results are presented in Figure 12. With an intervention rate of u_1 as shown in panel (f), we can observe a significant reduction in the number of infected individuals (see panel (b)), which is quite similar to the results of scenario 1 in Figure 11, panel (b). However, since the infection is transmitted through direct contact between plant and vectors, with no intervention applied to the vector population, we can observe the number of susceptible individuals as time progresses still decreases (see panel (a)). By the same argument, due to the substantial decrease in the number of infected hosts, panel (d) indicates that the number of susceptible vectors increases because infections

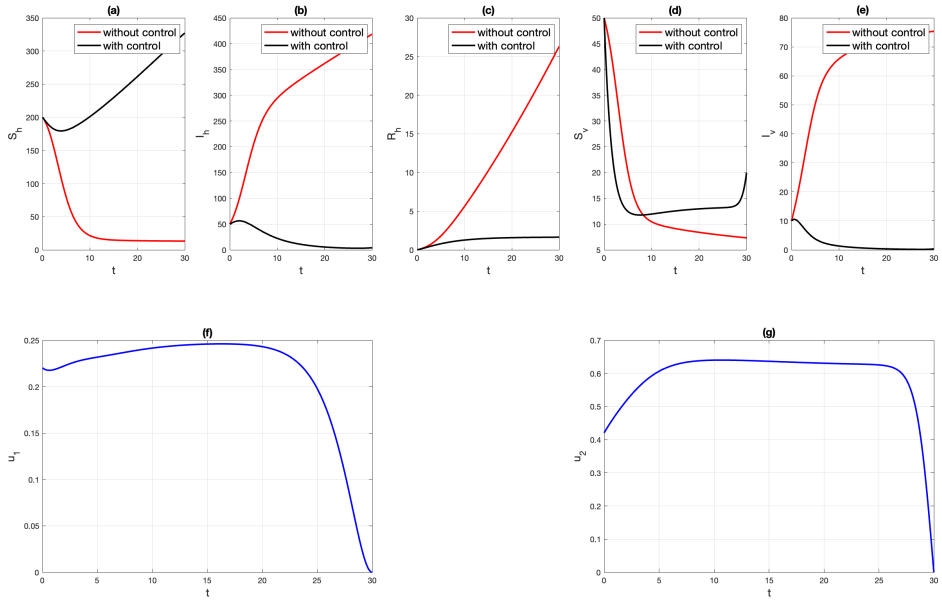

FIGURE 11. Simulation results for scenario 1

with infected plant occur less frequently. Although the intervention primarily focuses on the plant population, we can still see its impact on the number of infected vectors, even though it continues to increase. With maximum value of u_1 is 0.361 (larger than scenario 1), the cost function $\mathcal{J}$ for this scenario is 88.516.

Scenario 3. The last simulation is conducted to assess the impact of a vector-focused strategy, where $u_1 = 0$ and $u_2 \neq 0$. The results are presented in Figure 13. The dynamics of u_2 are depicted in panel (g), where the maximum value reaches 0.648, which is larger than that of scenario 1. As a result of this vector control intervention, the number of vectors is significantly reduced (see panels (d) and (e)), leading to a reduced number of infected plants (see panel (b)). The number of susceptible plants remains at a high level from the beginning of the simulation period (see panel (a)). The cost function $\mathcal{J}$ for this scenario is 213,677, which is the largest among all other scenarios.

4.4. Cost-effectiveness analysis. To analyze the most effective strategy between scenario 1, 2, and 3, it is necessary to analyze the cost-effectiveness for each scenario. To conduct this analysis, we calculate the Infected Averted Ratio (IAR) and Average Cost Effectiveness Ratio

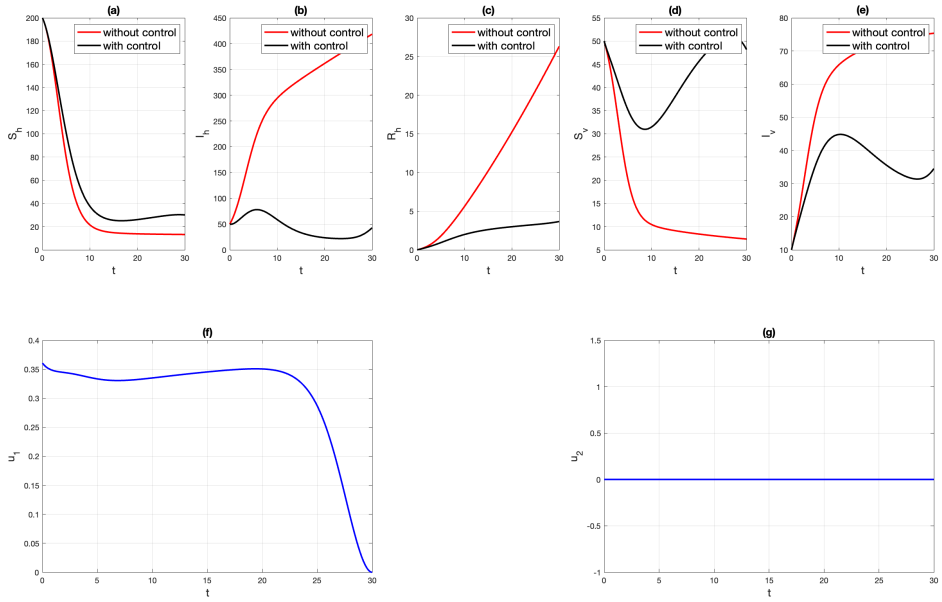

FIGURE 12. Simulation results for scenario 2

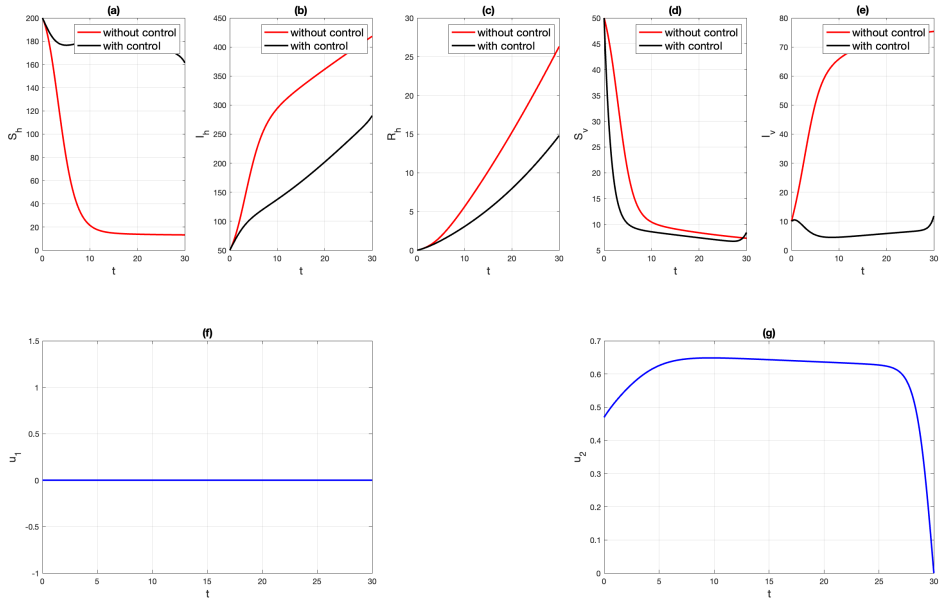

FIGURE 13. Simulation results for scenario 3

(ACER) for each scenario. IAR define as the ratio between total infection that been averted with the total number of recovered individuals [42]. This definition of IAR provides a measure of

the proportion of infections that have been averted or prevented compared to the total number of individuals who have recovered from the disease. It can be a useful metric for evaluating the effectiveness of interventions or treatments in reducing the burden of disease. Higher IAR values typically indicate a more successful intervention in preventing infections relative to the number of individuals who have recovered. From Table 2, Strategy 1 where u_1 and u_2 combined is the most effective strategy, followed by strategy 3 and 2, respectively.

TABLE 2. Infected averted (IA), Total cost of intervention (TC), Total Recovered (TR), Infected Averted Ratio (IAR), and Average Cost Effective Ratio (ACER). Blue and red represent the most and less effective strategy, respectively.

Scenario	IA	TC	TR	IAR	ACER
1: $u_1 \neq 0, u_2 \neq 0$	1.034×10^4	4.145×10^2	58.558	**176.7**	**0.040**
2: $u_1 \neq 0, u_2 = 0$	8.639×10^3	4.043×10^2	1.062×10^3	**8.127**	0.046
3: $u_1 = 0, u_2 \neq 0$	5.697×10^3	2.82×10^2	1.831×10^2	31.109	**0.049**

The Average Cost-Effectiveness Ratio (ACER) is a metric used in health economics and cost-effectiveness analysis to evaluate the cost-effectiveness of healthcare interventions or treatments [42]. In our case, it assesses the effectiveness of pruning u_1 and insecticide intervention u_2. ACER is defined as the ratio between the total cost of the intervention and the total number of infections averted due to the strategy. Therefore, ACER represents the average cost for each averted infection, with a smaller ACER indicating better cost-effectiveness. Looking at Table 2, we can once again observe that Strategy 1 is the most cost-effective, followed by Strategies 2 and 3, respectively

5. CONCLUSION

A mathematical model has been developed to depict the epidemiology of tungro disease in rice crops. This model incorporates two strategies for managing the spread of the virus: the application of insecticides to control the planthoppers that transmit the virus and the removal of infected rice plants. The model, which is a system of fifth-order non-linear differential equations, has two equilibria whose stability depends on the basic reproduction number. Local

stability analysis indicates that if the basic reproduction number is below one, the disease-free equilibrium is stable. Conversely, if the basic reproduction number exceeds one, the endemic equilibrium is guaranteed to exist and to be stable. This last condition has been proven numerically through a Monte Carlo simulation approach. An examination of the elasticity of the basic reproduction number provides valuable insight, indicating that insecticide application remains an effective method for controlling tungro, closely followed by the utilization of enhanced seeds. In addition, a number of potential control strategies for the tungro virus were evaluated. The results indicate that the most effective approach involves a dual strategy of using insecticides and removing infected rice plants. Another reliable option is to solely utilize insecticides. The proposed control strategy, specifically the integration of insecticide application alongside the removal of infected flora, can be employed as a comprehensive methodology in the management of Tungro disease within agronomic settings. This methodology is not solely efficacious in mitigating the propagation of the virus; it can concurrently assist agriculturalists in significantly reducing crop losses. The practical implications of this strategy suggest that disease management initiatives may leverage this framework to enhance the optimization of resources, including insecticides and labor, on a macro scale.

Data Availability Statement

The Python source code utilized in this study is publicly accessible. The code is accessible via GitHub at https://github.com/DaniSuandi174/spread_of_tungro_virus.git, and may be downloaded free of charge.

CRediT Authorship Contribution Statement

Dani Suandi: Writing – original draft, Methodology, Investigation, Formal analysis, Conceptualization, Supervision. Moch. Fandi Ansori: Writing – original draft, Visualization, Formal analysis. Dipo Aldila: Writing – original draft, Visualization, Formal analysis. Enceng Sobari: Investigation, Resources.Viska Noviantri: Writing – review & editing, Formal analysis. Nadirah binti Mohd Nasir : Writing – review & editing.

Acknowledgments

This work is supported by Bina Nusantara University as a part of Bina Nusantara University's BINUS International Research - Basic entitled *Investigation and Formulation of Optimal Strategies for the Control of the Spread of Infectious Diseases in the Agricultural Sector* with contract number: 096/VRRTT/VII/2024 and contract date 02 Juli 2024.

Conflict of Interests

The authors declare that there is no conflict of interests.

References

[1] G.S. Tanjung, A. Suryantini, A.W. Utami, The Priorities of Leading Sub-Sector in The Sector of Agriculture, Forestry, and Fisheries in Economic Development in Bangka Belitung Province, AGRARIS: J. Agribus. Rural Dev. Res. 7 (2021), 160–175. https://doi.org/10.18196/agraris.v7i2.11615.

[2] Y. Suzuki, I.G.N. Astika, I.K.R. Widrawan, et al. Rice Tungro Disease Transmitted by the Green Leafhopper: Its Epidemiology and Forecasting Technology, Japan Agric. Res. Quart. 26 (1992), 98-104.

[3] A. Niaz, M.M. Asad, A.A. Abdulmuhsin, et al. Risk Factors for the Rice Crop Farming Community in China: A Documentary Analysis of the Challenges During Post COVID-19, Asian Educ. Dev. Stud. 11 (2022), 298–310. https://doi.org/10.1108/aeds-11-2020-0257.

[4] B. Kalita, D. Hazarika, N. Rahman, P. Sarmah, Study on Crop Losses Due to COVID-19 Lockdown Period in Nagaon District of Assam: Crop Losses Due to COVID-19 Lockdown, J. AgriSearch 8 (2021), 167–172. https://doi.org/10.21921/jas.v8i2.7303.

[5] J. Beckman, A.M. Countryman, The Importance of Agriculture in the Economy: Impacts from COVID -19, Amer. J. Agric. Econ. 103 (2021), 1595–1611. https://doi.org/10.1111/ajae.12212.

[6] E. Loizou, C. Karelakis, K. Galanopoulos, K. Mattas, The Role of Agriculture as a Development Tool for a Regional Economy, Agric. Syst. 173 (2019), 482–490. https://doi.org/10.1016/j.agsy.2019.04.002.

[7] A. Kumar, B.S. Bhople, A. Kumar, R. Kapoor, B. Kumar, Impact-Losses, Reboot-Gain and Agricultural Effect during COVID-19 Pandemic, J. Sci. Res. Rep. 27 (2021), 1–6. https://doi.org/10.9734/jsrr/2021/v27i330364.

[8] S. Aday, M.S. Aday, Impact of COVID-19 on the Food Supply Chain, Food Qual. Safe. 4 (2020), 167–180. https://doi.org/10.1093/fqsafe/fyaa024.

[9] S. Pennazio, P. Roggero, M. Conti, Yield Losses in Virus-infected Crops, Arch. Phytopathol. Plant Protect. 30 (1996), 283–296. https://doi.org/10.1080/03235409609383178.

[10] S. Tatineni, G.L. Hein, Plant Viruses of Agricultural Importance: Current and Future Perspectives of Virus Disease Management Strategies, Phytopathology 113 (2023), 117–141. https://doi.org/10.1094/PHYTO-05-22-0167-RVW.

[11] K. Muralidharan, D. Krishnaveni, N. Rajarajeswari, et al. Tungro Epidemics and Yield Losses in Paddy Fields in India, Curr. Sci. 85 (2003), 1143-1147. https://www.jstor.org/stable/24108612.

[12] A. Jabeen, D. Subrahmanyam, D. Krishnaveni, Tungro Virus Disease in India: Historical Insights and Contemporary Prevalence Trends in Rice Cultivation, Agric. Arch. 2 (2023), 19–22. https://doi.org/10.51470/AGRI.2023.2.3.19.

[13] Y. Sun, D. Jing, J. Zhang, et al. Yield Components Affected by Rice Black-Streaked Dwarf Virus Disease in Rice Cultivars with Different Resistance Levels, Front. Microbiol. 14 (2023), 1323569. https://doi.org/10.3389/fmicb.2023.1323569.

[14] P. Teng, H. Hibino, H. Leung, Yield Loss Due to Rice Virus Diseases in Asian Tropics, Japan Int. Res. Center Agric. Sci. 22 (1988), 93–100.

[15] A.E. Voloudakis, A. Kaldis, B.L. Patil, RNA-Based Vaccination of Plants for Control of Viruses, Ann. Rev. Virol. 9 (2022), 521–548. https://doi.org/10.1146/annurev-virology-091919-073708.

[16] G. Dahal, A. Druka, T.M. Burns, L.C. Villegas, Z. Fan, R.B. Shrestha, R. Hull, Some Biological and Genomic Properties of Rice Tungro Bacilliform Badnavirus and Rice Tungro Spherical Waikavirus from Nepal, Ann. Appl. Biol. 129 (1996), 267–287. https://doi.org/10.1111/j.1744-7348.1996.tb05751.x.

[17] T.C.B. Chancellor, J.M. Thresh, (eds.) Epidemiology and Management of Rice Tungro Disease, Natural Resources Institute, Chatham, (1997).

[18] M.E. Abo, A.A. Sy, Rice Virus Diseases: Epidemiology and Management Strategies, J. Sustain. Agric. 11 (1997), 113–134. https://doi.org/10.1300/J064v11n02_09.

[19] C. Bragard, P. Caciagli, O. Lemaire, et al. Status and Prospects of Plant Virus Control Through Interference with Vector Transmission, Ann. Rev. Phytopathol. 51 (2013), 177–201. https://doi.org/10.1146/annurev-phyto-082712-102346.

[20] S.R. Dey, R. Das, M. De, A Brief Review on Present Status of Rice Tungro Disease: Types of Viruses, Vectors, Occurrence, Symptoms, Control and Resistant Rice Varieties, Int. J. Adv. Life Sci. Res. 07 (2024), 15–23. https://doi.org/10.31632/ijalsr.2024.v07i03.002.

[21] R.T. Hutasoit, M. Jihad, L. Listihani, et al. The Relationship between Vector Insect Populations, Natural Enemies, and Disease Incidence of Tungro Virus during Wet and Dry Seasons, Biodiversitas J. Biol. Divers. 24 (2023), 4001–4007. https://doi.org/10.13057/biodiv/d240737.

[22] T.C.B. Chancellor, A.G. Cook, K.L. Heong, The Within-Field Dynamics of Rice Tungro Disease in Relation to the Abundance of Its Major Leafhopper Vectors, Crop Protect. 15 (1996), 439–449. https://doi.org/10.1016/0261-2194(96)00002-6.

[23] O. Azzam, T.C.B. Chancellor, The Biology, Epidemiology, and Management of Rice Tungro Disease in Asia, Plant Dis. 86 (2002), 88–100. https://doi.org/10.1094/PDIS.2002.86.2.88.

[24] V. Nicaise, Crop Immunity against Viruses: Outcomes and Future Challenges, Front. Plant Sci. 5 (2014), 660. https://doi.org/10.3389/fpls.2014.00660.

[25] X.H. Truong, E.R. Tiongco, E.H. Batay-an, Rice tungro disease in the Philippines, in: T.C.B. Chancellor, O. Azzam, K.L. Heong, (eds.) Tungro Disease Management, pp. 1–10, 1999.

[26] A.A. Daradjat, N. Widiarta, A. Hasanuddin, Breeding for Rice Tungro Virus Resistance in Indonesia, in: T.C.B. Chancellor, O. Azzam, K.L. Heong, (eds.) Tungro Disease Management, pp. 31–38, 1999.

[27] L. Sebastian, E. Tiongco, D. Tabanao, et al. Breeding for rice tungro disease resistance at PhilRice, in: T.C.B. Chancellor, O. Azzam, K.L. Heong, (eds.) Tungro Disease Management, pp. 23–30, 1999.

[28] R. Cabunagan, E. Angeles, S. Villareal, et al. Multilocation Evaluation of Advanced Breeding Lines for Resistance to Rice Tungro Viruses, in: T.C.B. Chancellor, O. Azzam, K.L. Heong, (eds.) Tungro Disease Management, pp. 45–58, 1999.

[29] R. Amelia, N. Anggriani, A.K. Supriatna, N. Istifadah, Mathematical Model for Analyzing the Dynamics of Tungro Virus Disease in Rice: A Systematic Literature Review, Mathematics 10 (2022), 2944. https://doi.org/10.3390/math10162944.

[30] R. Amelia, N. Anggriani, A.K. Supriatna, N. Istifadah, Analysis and Optimal Control of the Tungro Virus Disease Spread Model in Rice Plants by Considering the Characteristics of the Virus, Roguing, and Pesticides, Mathematics 11 (2023), 1151. https://doi.org/10.3390/math11051151.

[31] R. Amelia, N. Anggriani, A.K. Supriatna, et al. Optimal Control Model for The Spread of Tungro Disease in Rice Plants by Controlling Using Pesticides, Eng. Lett. 32 (2024), 1097–1106.

[32] N.T. Blas, J.M. Addawe, G. David, A Mathematical Model of Transmission of Rice Tungro Disease by Nephotettix Virescens, AIP Conf. Proc. 1787 (2016), 080015. https://doi.org/10.1063/1.4968154.

[33] N. Blas, G. David, Dynamical Roguing Model for Controlling the Spread of Tungro Virus via Nephotettix Virescens in a Rice Field, J. Phys.: Conf. Ser. 893 (2017), 012018. https://doi.org/10.1088/1742-6596/893/1/012018.

[34] N. Anggriani, M. Yusuf, A.K. Supriatna, The Effect of Insecticide on the Vector of Rice Tungro Disease: Insight From a Mathematical Model, Information 20 (2017), 6197–6206.

[35] A. Maryati, N. Anggriani, E. Carnia, Stability Analysis of Tungro Disease Spread Model in Rice Plant Using Matrix Method, BAREKENG 16 (2022), 217–228. https://doi.org/10.30598/barekengvol16iss1pp215-226.

[36] W. Suryaningrat, N. Anggriani, A.K. Supriatna, Mathematical Analysis and Numerical Simulation of Spatial-Temporal Model for Rice Tungro Disease Spread, Commun. Math. Biol. Neurosci. 2022 (2022), 44. https://doi.org/10.28919/cmbn/7160.

[37] W. Suryaningrat, N. Anggriani, A.K. Supriatna, N. Istifadah, The Optimal Control of Rice Tungro Disease with Insecticide and Biological Agent, AIP Conf. Proc. 2264 (2020), 040002. https://doi.org/10.1063/5.0023569.

[38] M.J. Jeger, J. Holt, F. Van Den Bosch, L.V. Madden, Epidemiology of Insect-transmitted Plant Viruses: Modelling Disease Dynamics and Control Interventions, Physiol. Entomol. 29 (2004), 291–304. https://doi.org/10.1111/j.0307-6962.2004.00394.x.

[39] A. Perasso, An Introduction to The Basic Reproduction Number in Mathematical Epidemiology, ESAIM: Proc. Surv. 62 (2018), 123–138. https://doi.org/10.1051/proc/201862123.

[40] J.A.P. Heesterbeek, A Brief History of R_0 and a Recipe for its Calculation, Acta Biotheor. 50 (2002), 189–204. https://doi.org/10.1023/A:1016599411804.

[41] D. Suandi, M.A. Ginting, Monte Carlo Simulation Method in Stability Analysis of Epidemiological Models, Commun. Math. Biol. Neurosci. 2024 (2024), 135. https://doi.org/10.28919/cmbn/8971.

[42] D. Aldila, Optimal Control for Dengue Eradication Program under the Media Awareness Effect, Int. J. Nonlinear Sci. Numer. Simul. 24 (2023), 95–122. https://doi.org/10.1515/ijnsns-2020-0142.